Environmental assessment of metal-organic framework DUT-4 synthesis and its application for siloxane removal

Sandra Pioquinto-García[†§], *Juana María Rosas*[§], *Margarita Loredo-Cancino*[†], *Sylvain Giraudet*[†,‡], *Eduardo Soto-Regalado*[†], *Pasiano Rivas-García*[‡*], *Nancy E. Dávila-Guzmán*[†*].

[†] Facultad de Ciencias Químicas, Universidad Autónoma de Nuevo León, UANL, Av. Universidad S/N, Cd. Universitaria, San Nicolás de los Garza, Nuevo León, 66455, México.

‡Centro de Investigación en Biotecnología y Nanotecnología, Facultad de Ciencias Químicas, Universidad Autónoma de Nuevo León. Parque de Investigación e Innovación Tecnológica, km 10 Highway to the International Airport Mariano Escobedo, Apodaca, Nuevo León, 66629, México.

[§] Departamento de Ingeniería Química, Facultad de Ciencias, Universidad de Málaga, Andalucía TECH, Campus de Teatinos s/n, Málaga, 29010, Spain.

[†,‡] Ecole Nationale Supérieure de Chimie de Rennes, 11 Allée de Beaulieu, 35708 Rennes, France.

Corresponding Authors

* Nancy Elizabeth Dávila-Guzmán, **E-mail:** nancy.davilagz@uanl.edu.mx, **Phone number:** 52-8183294000, ext. 3475

* Pasiano Rivas García, **E-mail:** pasiano.rivasgr@uanl.edu.mx

KEYWORDS: Adsorption; Life cycle assessment; Biogas; Octamethylcyclotetrasiloxane; Kinetics of adsorption.

ABSTRACT

Metal-organic frameworks (MOF) have been used for gas storage, catalysis, and adsorption. Commonly, MOF are activated by solvent evaporation to achieve high surface areas and better performances. However, MOF synthesis has been criticized for the consumption of non-green solvents. Therefore, a technical and environmental study of solvothermal and hydrothermal synthesis of MOF DUT-4 was developed in this work. The technical study considered the siloxane adsorption of DUT-4 for biogas purification, and the environmental study was implemented using the life cycle assessment (LCA) methodology. The results indicated that technically similar materials are obtained through solvothermal synthesis. The siloxane adsorption capacity for the materials obtained by solvothermal and hydrothermal synthesis was 9.80 and 1.80 mg/g, respectively. Based on the LCA, most of the environmental damage from DUT-4 solvothermal synthesis depended on the use of solvents in the synthesis, cleaning, and solvent exchange stages (up to 244 mPt). Although the use of non-green solvent dimethylformamide in the DUT-4 production increased the environmental impacts, its high adsorption capacity causes the lowest environmental impact/adsorption capacity ratio (11.44). Thus, the best DUT-4 production route that considers both low environmental impact and high

adsorption capacity of siloxane was the solvothermal synthesis of DUT-4 with a non-solvent exchange.

INTRODUCTION

Renewable energies have been the focus of attention among countries due to the continuous increases in the price of fossil fuels and the need to environmental care. Biogas is a green energy source that is used as a cleaner transportation fuel [1]. Basically, the biogas is a mixture of methane (35–70 %), carbon dioxide (15–50 %), and small amounts of undesirable compounds (<2 %) such as H_2S (~1560 ppmv), NH_3 (~91 ppmv), CO (~416 ppmv), H_2 (~367 ppmv), moisture, and volatile compounds [2-5].

Among the volatile compounds found in biogas, the siloxanes are of great interest since they have adverse effects on combustion systems. After combustion, the siloxanes decompose into two new products: formaldehyde and orthosilicic acid [6], these products form a soft paste that contributes to abrasion, metal friction, and failure of mechanical elements of the combustion system.

The necessity of siloxane removal from biogas is a priority for advancing the energy recovery potential of biogas. Current technologies for siloxane removal from biogas include adsorption, absorption, cryogenics, separation by membranes, and biological processes [7-10]. Nevertheless, the adsorption process with activated carbon (AC) is the most used siloxane removal technique due to its relatively low acquisition cost [10-12] and efficiency (90–99 %), achieving the siloxanes concentration up to 0.1 mg/m^3 in the biogas [9]. The main drawback of using AC for this purpose is the high regeneration temperature (>400 ºC), causing high operation costs.

Accordingly, new adsorbent materials as the metal-organic frameworks (MOF) have been recently developed to overcome the shortcomings of several conventional adsorption processes.

MOF are porous materials formed by metal centers linked with organic ligands (coordination compounds). Depending on the geometric characteristics of the metallic units and the organic ligands of the MOF, it will be its type of permanent pore and cavity. Due to high porosity and surface area, easy modification, thermal stability, and regeneration [13]; MOF have been widely used in catalysis, gas adsorption [14,15], optics, magnetism [13], and chemical sensors [16]. Recently, Mito-oka et al. [17] employed the MOF developed by Dresden University Technology 4 (DUT-4) and conventional AC for siloxane adsorption. The results showed that even in wet conditions, the DUT-4 has high selectivity and uptake compared to AC performance. The DUT-4 removal efficiency at 30ºC was higher than 90 %, and the AC removal efficiency was 70 % at 500 min. of operation. The DUT-4 removal efficiency was attributed to its strong hydrophobicity and optimal chemical interactions with siloxane octamethylcyclotetrasiloxane (D4). Secondly, Gargiulo et al. [18] demonstrated the high affinity of the MOF MIL-101(Cr) for the removal of siloxane D4 as well as the complete regeneration of this adsorbent at moderated temperature (150 ºC). The authors indicated that contrary to AC and silica gel (SG), D4 removal by MIL-101(Cr) does not cause polymerization of D4 on the adsorbent surface, which allowed its reusability.

Although MOF have been pointed out as "green materials" for sustainable processes, the environmental impact of their synthesis has been barely evaluated. The life cycle assessment (LCA) is a methodology that can determine how green a material is [19]. LCA has been used by Loya-González et al. [20] and Sepúlveda-Cervantes et al. [21] to determine the impacts of some adsorbents materials such as AC synthesized from biomass waste. In such works, the

impregnation stage of the AC production was found to be the largest contributor to environmental damage, owing to the high energy consumption of this stage and the use of chemicals such as $ZnCl_2$ and KOH.

To the best of our knowledge, there is not one study in the literature about using LCA to synthesize MOF to cleaning biogas. Grande et al. [22] evaluated the environmental impact of the MOF CPO-27-Ni synthesized by four different routes. They found that the main contributors to the environmental impact of CPO-27-Ni were the synthesis and cleaning stages, mainly associated with the toxicity of tetrahydrofuran and dimethylformamide. When water was used in the synthesis or cleaning stage, the environmental impact was reduced from 1136.2 to 12.3 kg CO_2 eq per kg of MOF.

In the literature, a study of the environmental impact of the MOF DUT-4 has not been identified, and this is of particular interest because DUT-4 is a promising material for cleaner biogas production. This work aims to evaluate the environmental impact of the DUT-4 with the LCA methodology, proposing alternatives to reduce its environmental impact.

MATERIALS AND METHODS

DUT-4 synthesis routes

Synthesis of DUT-4(DMF). The synthesis of DUT-4(DMF) was performed with some variations as described by Senkovska et al. [23]: 0.26 g of 2,6-naphthalene dicarboxylic acid was dissolved in 30 mL of N,N-dimethylformamide (DMF); subsequently, 0.52 g of nonahydrate aluminum nitrate was added and mixed. The mixture was poured into a 250 mL Teflon liner and placed in an autoclave at 120 ºC for 24 h. At the end of this time, it was cooled to room

temperature. The product was centrifuged at 10,000 rpm and 2.5 min, then washed three times with DMF, and finally dried in an oven at 120 ºC for 4 h.

Synthesis of DUT-4(DCM). The synthesis of DUT-4(DCM) was carried out by including a solvent exchange step in the synthesis of DUT-4(DMF), adding 20 mL of dichloromethane (DCM) for 1 h (20 min each wash). The product was then centrifuged at 10,000 rpm for 2.5 min and dried in an oven at 120 ºC for 4 h.

Synthesis of DUT-4(H). In the synthesis of DUT-4(H), a second solvent exchange stage was included, consisting of three washes with 20 mL of hexane (C_6H_{14}) per 1 h (20 min each wash). The product was centrifuged and dried in the same way as in the previous synthesis.

Synthesis of DUT-4(W). This synthesis was carried out using deionized water instead of DMF to contribute to a greener production.

Characterization techniques of the adsorbents

Physicochemical characterization. X-ray diffraction patterns (XRD) were recorded on a PANalytical X'Pert PRO MPD diffractometer using Cu-Kα radiation (40 mA and 45 kV); the relative crystallinity was determined by the area under the curve of the crystalline peaks (after baseline correction). The specific surface area (A_s) of DUT-4 were obtained by N_2 physisorption at 77 K using a Micromeritics ASAP 2020 after out-gassing the DUT-4 at 150 ºC for 8 h. Solid-state ^{27}Al MAS NMR spectra were recorded at room temperature in a Bruker AVANCE III HD 600 MHz NMR spectrometer at 20 kHz, with a length pulse of 0.27 μs and a 1 s delay with 1H decoupling and summing up 2000 scans. Scanning electron microscopy (SEM) images were obtained using a JEOL JSM-6490LV microscope with acceleration voltage from 0.3 to 30 kV

and thermionic electron gun with W filament. FTIR spectra were obtained from a Bruker Tensor 27 using a Golden Gate Single Reflection diamond ATR cell and a standard spectral resolution of 4 cm^{-1} in the spectral range of 4000–500 cm^{-1}.

Adsorption experiments. The adsorption experiments were carried out at 450 mg/Nm^3 of initial concentration of D4, 100 mg of adsorbent material, and room temperature. Flasks were stirred at 700 rpm for 6–9 h to ensure equilibrium. During the adsorption experiments, the samples were analyzed for D4 concentration through gas chromatography. Each sample was injected into a Shimadzu Nexis GC-2030 gas chromatograph with a flame ionization detector (FID) to measure the concentration of siloxane D4. The column used was SH-Rxi-5ms Shimadzu capillary column (15 m x 0.25 mm inner diameter x 0.25 µm film thickness). The inlet oven and detector temperature were set at 150, 110, and 250 °C, respectively. Helium was used as carrier gas at a constant flow rate of 1.5 mL/min and 83.3 kPa. The injected volume was 0.5 mL with split radio 5.0, and the duration of the method was 1.4 min. The adsorption capacity was determined by mass balance as follows:

$$q = \frac{(C_o - C)V}{m} \qquad \text{Eq. (2)}$$

where q is the adsorption capacity (mg/g), C_o is the D4 initial concentration (mg/Nm^3), C is the D4 concentration over time (mg/Nm^3), V is the volume (m^3), and m is the adsorbent mass (g).

Life cycle assessment implementation

Goal and scope definition of the product system. The LCA of the DUT-4 production process in laboratory-scale was carried out according to ISO 14044 [24]. The system boundary for DUT-4 includes five stages: mixing, synthesis, cleaning, solvent exchange, and drying (Figure 1). In

this analysis, the environmental burdens associated with the laboratory equipment construction used in the production of DUT-4 were not considered. Each of the different DUT-4 synthesis strategies was considered as study scenarios:

- Scenarios DUT-4(DMF) and DUT-4(W): include the stages of mixing, synthesis, cleaning, and drying.

- Scenarios DUT-4(DCM) and DUT-4(H): include additionally the solvent exchange stage due to exchanges with different solvents.

Such scenarios are represented in the system boundaries as shown in Figure 1. The functional unit (FU) was defined as the production of 1 g of DUT-4 produced on a laboratory scale. According to other LCA studies of adsorbents materials, the FU unit was established on a mass basis, such as activated carbon and MOF-74 [21], [22].

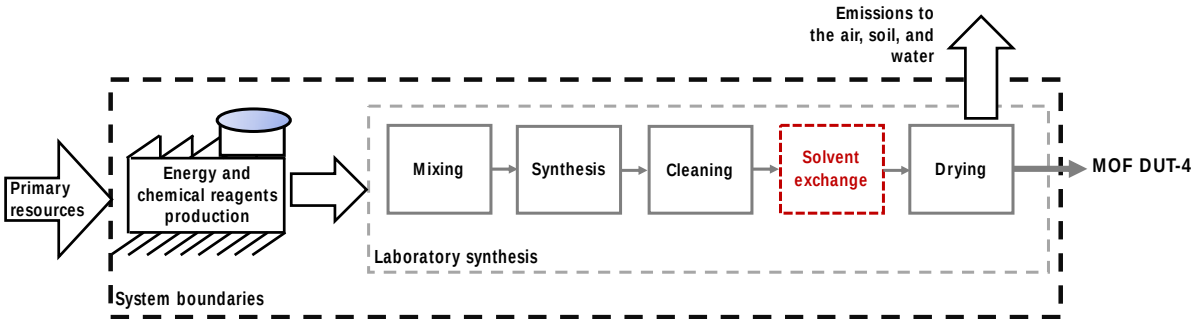

Figure 1. System boundaries for the production of DUT-4.

Life cycle inventory analysis. The data for the life cycle inventory (LCI) of chemical reagents and energy used in the scenarios for DUT-4 synthesis were obtained from the laboratory logs, analytical procedures, and material-energy balances. The production of energy and chemical reagents needed to synthesize DUT-4 was considered inside the system boundaries. The LCI for

these resources was taken from the Ecoinvent v3.3 database [25]. The wastewater generated in the cleaning stage was disposed of according to the hazardous waste management program implemented in our university [26]. Therefore, the environmental impacts of the final disposal of this waste were not considered in the LCI, as reported by Loya-González et al. [20] and Sepúlveda-Cervantes et al. [21].

The life cycle stages of DUT-4 production that demand energy were synthesis, cleaning, solvent exchange, and drying. The energy requirement in the synthesis stage was calculated by an energy balance (Figure S1, Table S1). The details of the energy balance are present in Section S1 of the supplementary material. The cleaning and solvent exchange stages include the separation of the solvent by centrifugation. The energy consumption in these stages was calculated by the rotational kinetic energy equation presented according to Section S2. The energy required in the drying stage was obtained by calculating the heat energy required to remove the solvent per unit mass of DUT-4. The energy balance for this stage was taken from Sepúlveda-Cervantes et al. [21]; the parameters used are specified in the Table S2 of the Section S3. During the drying stage of study scenarios, DMF, DCM, hexane, and water are released into the atmosphere. Gravimetric analysis was carried out to estimate the mass of these emissions. The DUT-4 sample was weighed before and after being dried in an oven at 120 °C for 4 h. The weight difference was related to the emission of the solvent from the DUT-4.

This LCI was carried out following an attributional approach. This perspective aims to quantify the environmental impacts attributed to the production system. It is based on evaluating the emission and resource flows that accompany the product as it moves through its life cycle, applying representative average data for all processes and input and output flows involved in the life cycle [27].

Life cycle impact assessment. The life cycle impact assessment (LCIA) model was constructed using the LCA software SimaPro 7.3.3 (PRe Consultants, Amers-foort, the Netherlands). The LCIA was performed according to the ReCiPe 2016 method [28], considering midpoint and endpoint indicators.

RESULTS AND DISCUSSIONS

Physicochemical characterization

The FTIR spectrum of DUT-4(DMF), DUT-4(DCM), DUT-4(H), and DUT-4(W) showed similar adsorption bands (Figure 2). The band in the range 1693–1668 cm^{-1} in each of the spectra corresponding to the stretching vibration of (ν(C=O)) of the carbonyl group, which is indicative of the coordination of linker to the metal ion [29]. The band in each spectrum at 1614–1598 cm^{-1} corresponded to asymmetric stretching vibrations of carboxylate group (ν_{as}(C-O)) [30]; the bands in the range of 1434–1415 cm^{-1} corresponded to symmetric stretching vibrations of carboxylate group (ν_{s}(C-O)), and the peaks observed at 989–985 cm^{-1} are related to the bending of the bridging groups δ(O-H) [31]; the bands between 792 and 783 cm^{-1} in each of the spectra corresponded to flexions into the aromatic plane [32], [33], and the bands between 586–561 cm^{-1} in the four spectra were associated with the stretching vibrations of the aluminum atom with oxygen atoms (ν(Al-O)) [34]. Additionally, in the DUT-4(W) spectrum, the band at 1294 cm^{-1} was associated with the (ν(C-O)) stretch vibration, and the bands at 921–914 cm^{-1} were due to the (δ(O-H)) bend [35].

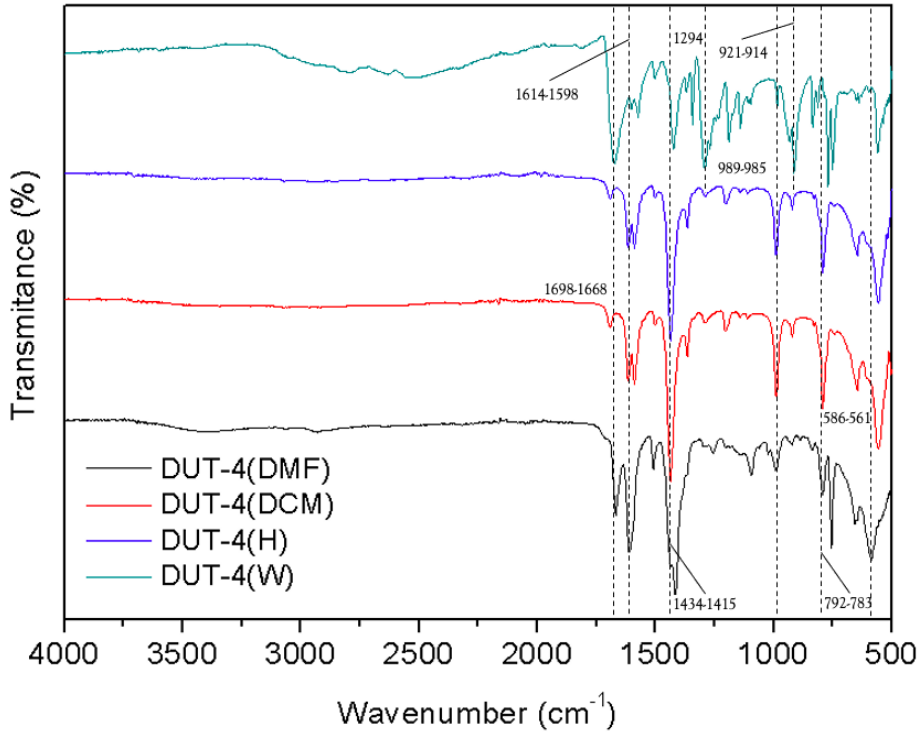

Figure 2. FTIR/ATR spectra for DUT-4(DMF), DUT-4(DCM), DUT-4(H), and DUT-4(W).

Solid-state ^{27}Al MAS NMR spectroscopy can be used for MOF characterization to determine the local chemical environment and the coordination state of the metal sites. Here, the ^{27}Al MAS NMR spectra for DUT-4(DMF), DUT-4(DCM), DUT-4(H), and DUT-4(W) were obtained (Figure 3). The primary resonating signal of all the materials studied corresponded to 6-fold coordinated aluminum sites ($Al^{[6]}$) [36], [37], with three overlapped signals in the chemical shift range between -20 to 10 ppm as reported by Volkringer et al. [38] for the Al-MIL-100 structure. According to Vyalikh et al. [39], differences in aluminum sites are due to coordination with distinct types of OH groups. That is, each aluminum site is coordinated to different OH-groups that participate in intralayer and interlayer hydrogen bonds, causing changes in the chemical

environment. Altogether, the NMR spectra for DUT-4 demonstrate the presence of octahedral aluminum sites in the MOF structure.

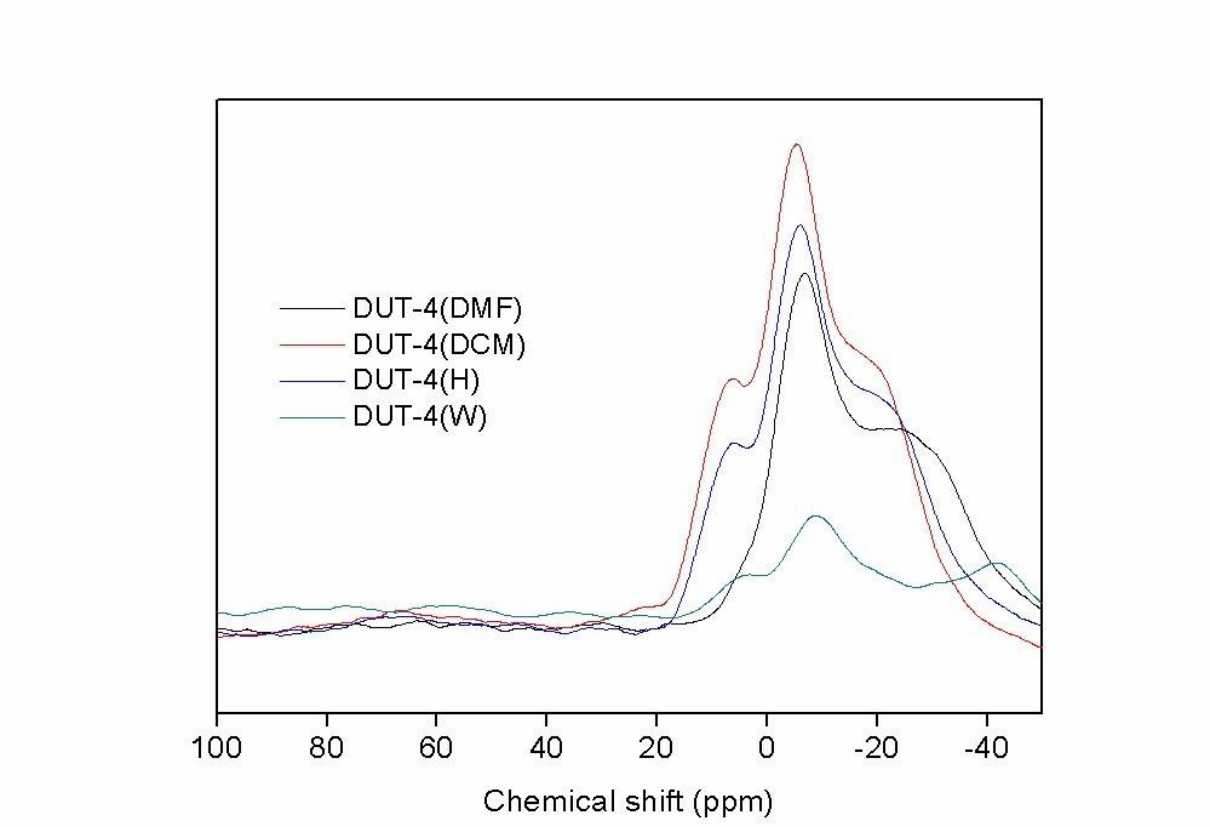

Figure 3. ^{27}Al MAS NMR Spectra for DUT-4(DMF), DUT-4(DCM), DUT-4(H), and DUT-4(W).

The diffraction patterns of as-synthesized samples of DUT-4 by solvothermal synthesis shown characteristic peaks at 6.95º, 13.91º, and 21.04º corresponding to (101), (110), and (113) Miller indices, respectively, and an orthorhombic symmetry according to Senkovska et al. [23]. A significant increase in the relative intensity of the diffraction Bragg peaks was observed on the XRD pattern of DUT-4(DCM) and DUT-4(H) compared to DUT-4(DMF). The calculated crystallinity percentages were 70.82 %, 89.26 %, and 88.74 % for DUT-4(DMF), DUT-4(DCM), and DUT-4(H), respectively. These results suggest that the use of low surface tension solvents

instead of DMF improves the crystallinity of the MOF and prevents structural collapse [40]. To continue, the hydrothermal synthesis of DUT-4(W) allowed to obtain a structure with 89.89 % crystallinity but non-isostructural to DUT-4 (Figure 4). The higher intensity peaks of the DUT-4(W) phase were 16.39º and 27.74º which are similar to the organic linker 2,6-naphthalene dicarboxylic acid [41]. It has been reported that water molecules can prevent the coordination between the organic linkers and the ion atoms by hydrogen bonding interactions with the organic linkers [42].

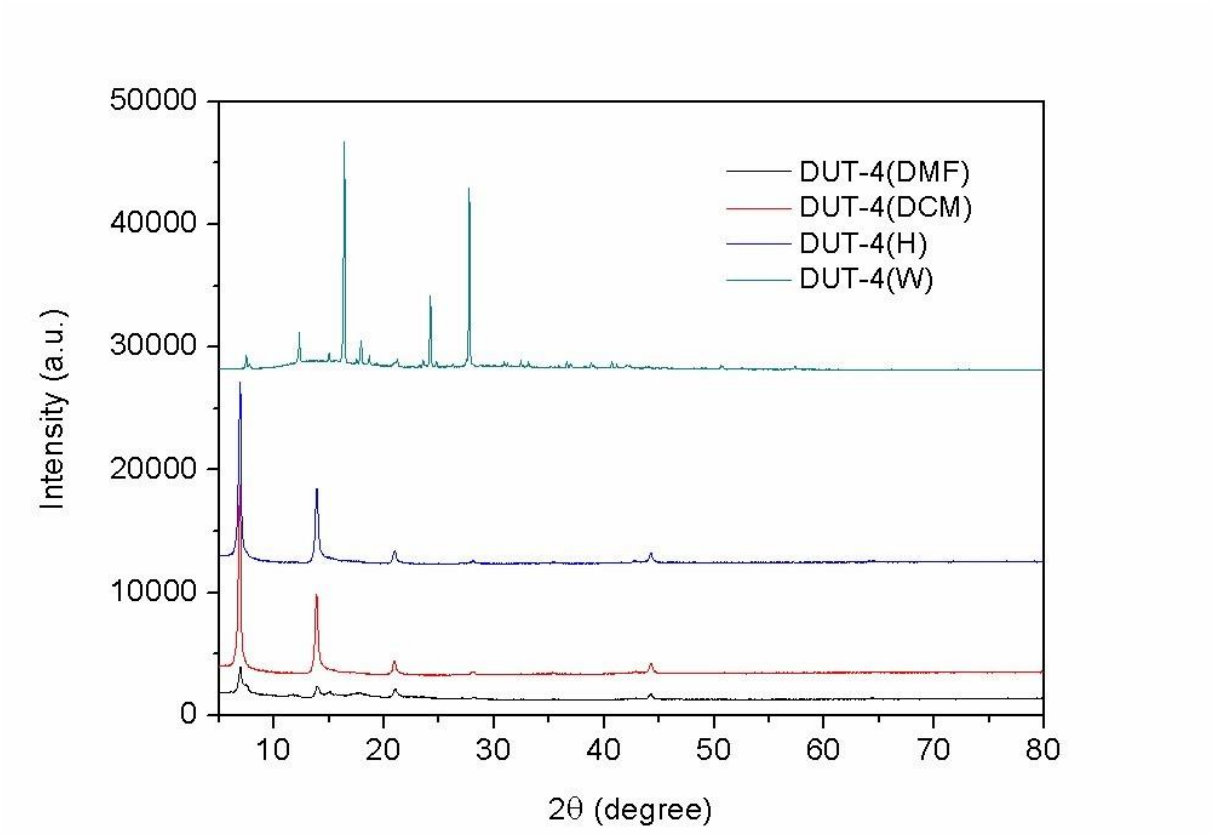

Figure 4. XRD pattern obtained from DUT-4(DMF), DUT-4(DCM), DUT-4(H), and DUT-4(W) powders.

The specific surface area of the synthesized DUT-4(DMF) had a similar value (1348 m^2/g) to that reported by Senkovska et al. [23] (1308 m^2/g). According to Howarth et al. [43], the solvent

exchange with low surface tension solvents helps to achieve the highest possible surface area and porosity. Accordingly, a solvent exchange of DMF for CH_2Cl_2 was carried out to obtain the DUT-4(DCM) material, although a slight reduction of 12 % of the A_s was observed (1184 m^2/g). To overcome this reduction on the A_s, DUT-4(DCM) was subjected to a second solvent exchange process where DCM was exchanged for C_6H_{14}, and the as-synthesized material was named DUT-4(H). The specific surface area of DUT-4(H) (1335 m^2/g) was very similar to that obtained for DUT-4(DMF). Thus, by solvothermal synthesis, irrespective of the solvent exchange, high specific surface areas were obtained. The total pore volume for DUT-4(DMF), DUT-4(DCM), and DUT-4(H) were 1.71, 1.48, and 1.46 cm^3/g, respectively. Differently, a hydrothermal synthesis was carried out to use a greener solvent such as water instead of the toxic DMF solvent, however, low specific surface area was obtained (1.78 m^2/g) as well as low total pore volume (0.003 cm^3/g). Usually, water-based MOF has low porosity in comparison with MOF obtained by solvothermal synthesis [44].

The particle size of the materials obtained by solvothermal synthesis was dependent on the solvent used in the drying stage. When low surface tension solvents were used (DCM, 29.5 and H, 18.8 dyn/cm), a small particle size was obtained. For instance, DUT-4(DCM) and DUT-4(H) particle size was lower than 500 nm. Conversely, when a high surface tension solvent such as DMF (37.9 dyn/cm) was used, the particle size of DUT-4(DMF) was greater than 1 μm (Figure 5). Similar results were obtained for the hydrothermal synthesis (H_2O, 72.8 dyn/cm), where particles of different sizes exceeding 3.25 μm were found. The formation of larger agglomerates during drying of the DUT-4(DMF) and DUT-4(W) was due to the capillary forces overcoming the repulsive forces between the particles; therefore, the particles came closer to each other [45,46].

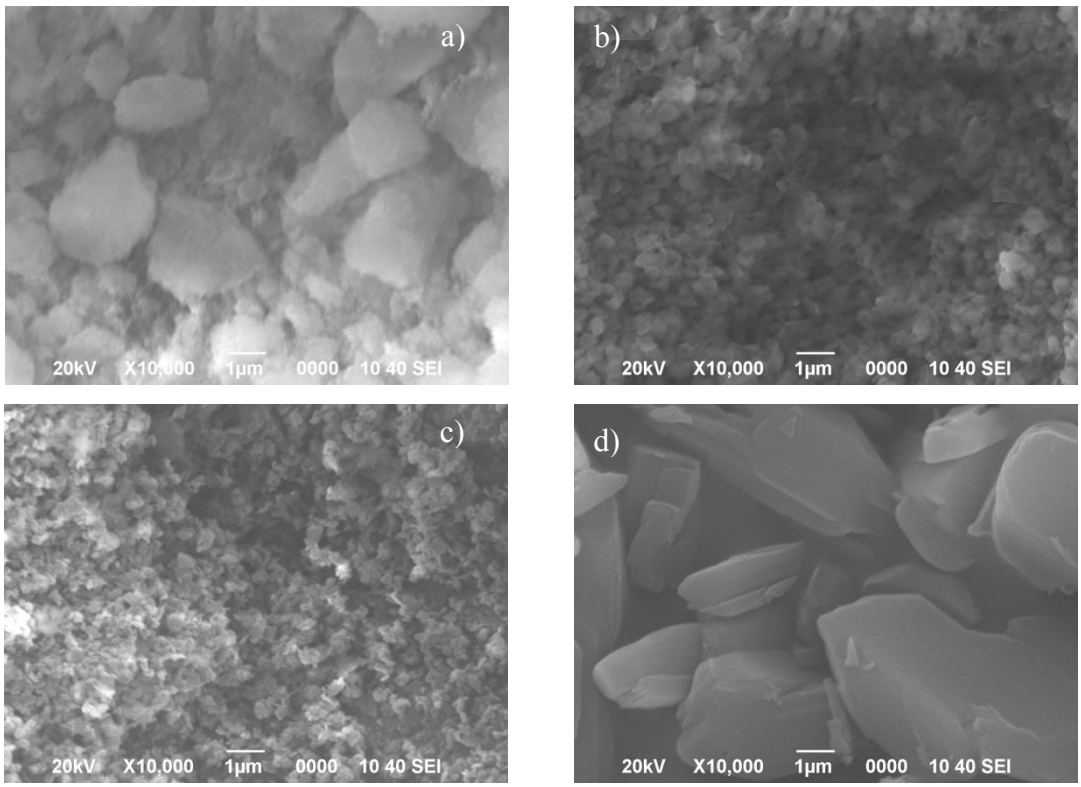

Figure 5. SEM image for a) DUT-4(DMF), b) DUT-4(DCM), c) DUT-4(H), and d) DUT-4(W).

In summary, according to the FTIR and NMR analysis, the materials obtained by both solvothermal and hydrothermal synthesis shown the characteristics absorption bands of the functional groups of the organic linker and the chemical shifts related to the six-fold coordinated Al, respectively. The four synthesized materials presented a crystalline structure with values between 70–90 % but only the solvothermal synthesis produced materials isostructural to DUT-4. In addition, high specific surface areas with values higher than 1100 m^2/g were obtained by solvothermal synthesis. Meanwhile, the hydrothermal synthesis generated a low specific surface area and low total pore volume caused by high surface tension solvent. Similarly, the solvent used on the drying stage affected the particle size of the studied materials. That is, low surface tension solvent leads to a small particle size. The trend on the particle size was DUT-4(H)≈ DUT-4(DCM) <DUT-4(DMF) <DUT-4(W) which is similar to the trend of the surface

tension of solvents: C_6H_{14} (18.8 dyn/cm) <Cl_2CH_4 (29.5 dyn/cm) <DMF (37.9 dyn/cm) <H_2O (72.8 dyn/cm).

Adsorption. The adsorption experiments were carried out at an initial concentration of 450 mg/Nm^3 of siloxane D4 at room temperature. The kinetic adsorption of the DUT-4 materials was rapid, reaching equilibrium about 4 h (Figure 6). The equilibrium adsorption capacity for DUT-4(DMF), DUT-4(DCM), and DUT-4(H) was 9.80 mg/g, which is 1.4 times greater than the adsorption capacity of AC (A_s 1240 m^2/g) reported in our previous work under the same experimental conditions [47]. The siloxane adsorption during the first hour was higher for DUT-4(DCM) than for DUT-4(H), which is related to the adsorption kinetics rate. Thus, a simple approach was made to quantify the adsorption kinetics rate by calculating the slope of the first experimental points (from zero to one hour). According to the experimental data, the adsorption rate followed the trend of DUT-4(DCM) <DUT-4(DMF) <DUT-4(H) with values of 7.09, 6.54, and 5.08 mg/g·h, respectively. On the other hand, the adsorption capacity of DUT-4(W) was 1.80 mg/g, reaching equilibrium in 2 h and was five times less than the adsorption capacity of the rest of DUT-4 adsorbents, associated with its low specific surface area (1.78 m^2/g).

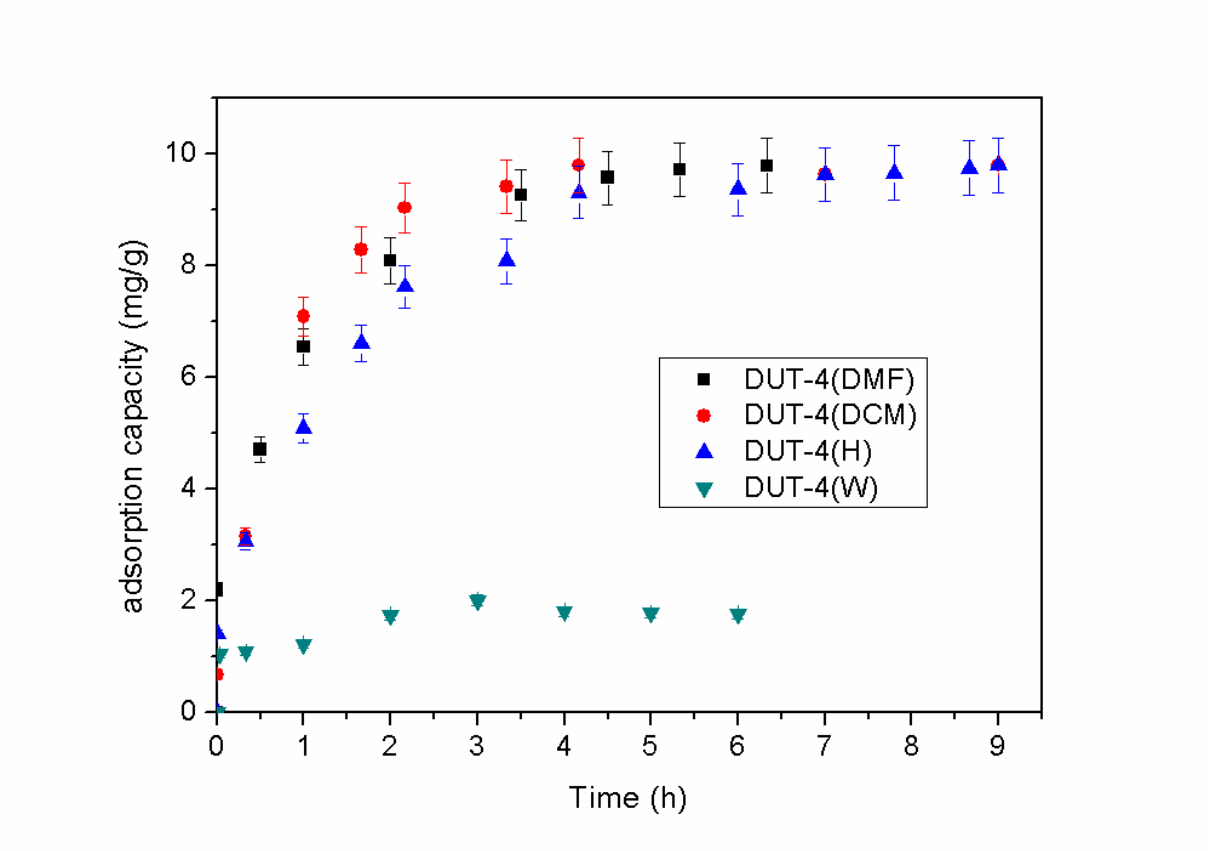

Figure 6. Kinetics adsorption for DUT-4(DMF), DUT-4(DCM), DUT-4(H), and DUT-4(W) at the initial concentration of D4 of 450 mg/Nm^3 and room temperature.

Life cycle inventory of DUT-4 production. The inputs and outputs flow in the production of DUT-4 are detailed in Table 1. According to these data, the use of chemical reagents to produce DUT-4 generated the highest environmental impact with a single score between 88.6 and 245 mPt (79.1 and 91.1 % of total environmental damage), while the electrical energy consumption generated a single score between 2.12 and 24.7 mPt, except for scenario DUT-4(W), where the electricity consumption generated 31.6 mPt while the use of chemical reagents caused 0.66 mPt. These results were similar to the obtained by other authors who evaluated the synthesis of adsorbent materials on a laboratory scale. The production of inputs (chemical reagents) comprises the activities with the most significant environmental damage. Loya-González et al.

[20] and Sepúlveda-Cervantes et al. [21] found that, for the single score indicator (determined through the ReCiPe 2008 method [48]), the production of chemical inputs represents between 93, and 83-93 % of the total environmental damage in the production of activated carbon from agro-industrial waste, respectively. Hjaila et al. [49] found that the production of phosphoric acid contributes more than 90 % to the midpoint indicators of human toxicity and terrestrial acidification (evaluated through the CML 2 Baseline 2000 method [50]) for the production of activated carbon from olive-waste cakes.

Table 1. Inventory data for DUT-4 production.

FLOW	**VALUE**	**UNITS/FU**
Inputs		
Electricity		
Synthesis stage (for all scenarios)	211	W-h
Cleaning and solvent exchange stage		
Scenario DUT-4(DMF)	70	W-h
Scenario DUT-4(DCM)	90	W-h
Scenario DUT-4(H)	80	Wh
Scenario DUT-4(W)	160	Wh

Drying

Scenario DUT-4(DFM)	2	Wh
Scenario DUT-4(DCM)	4	Wh
Scenario DUT-4(H)	2	Wh
Scenario DUT-4(W)	9	Wh

Chemical reagents

Mixing/synthesis

N, N-Dimethylformamide:

Scenario DUT-4(DMF)	65.2	mL
Scenario DUT-4(DCM)	103	mL
Scenario DUT-4(H)	111	mL
Scenario DUT-4(W)	162	mL

2,6-Naphthalene dicarboxylic acid:

Scenario DUT-4(DMF)	0.56	g
Scenario DUT-4(DCM)	0.90	g

Scenario DUT-4(H)	0.96	g
Scenario DUT-4(W)	1.41	g

Nonahydrate aluminum nitrate:

Scenario DUT-4(DMF)	1.13	g
Scenario DUT-4(DCM)	1.79	g
Scenario DUT-4(H)	1.93	g
Scenario DUT-4(W)	2.81	g

Cleaning

N, N-Dimethylformamide:

Scenario DUT-4(DMF)	130	mL
Scenario DUT-4(DCM)	207	mL
Scenario DUT-4(H)	222	mL
Deionized water-Scenario DUT-4(W)	325	mL

Solvent exchange

Dichloromethane:

Scenario DUT-4(DCM)	207	mL
Scenario DUT-4(H)	222	mL
Hexane-Scenario DUT-4(H)	222	mL
Outputs		
Emissions (Drying stage)		
Scenario DUT-4 (DMF), dimethylformamide	2.7	g
Scenario DUT-4(DCM), dichloromethane	9.8	g
Scenario DUT-4(H), hexane	4.5	g
Scenario DUT-4(W), H_2O	4.03	g

FU: functional unit

Environmental impacts of DUT-4 production. All environmental impact results are related to FU. Figure 7 presents the environmental impact assessment results for each Scenario of DUT-4 production through the ReCiPe 2016 endpoint method. Scenario DUT-4(H) has the highest single score of 269 mPt, due to the environmental impact in the cleaning and solvent exchange stages, where three types of solvents were used: DMF, DCM, and hexane. The use of these solvents also increases the cleaning stage's energy demand (Table 1) because the use of each solvent requires centrifugation. Altogether, solvent production contributes to 245 mPt in

Scenario DUT-4(H), 61.5 %, 33.3 %, and 5.2 % to DMF, DCM, and hexane. The use of these three solvents in Scenario DUT-4(H) led it to be the leader in all the environmental impact indicators (Figure S2). Due to the fact that same adsorption capacities (9.8 mg/g) were obtained by the three adsorbents DUT-4(DMF), DUT-4(DCM), and DUT-4(H), it is possible to propose a cleaner and greener DUT-4 production by avoiding additional solvents such as DCM and H. In this manner, principles 3, 4, and 5 of green chemistry are fulfilled [51].

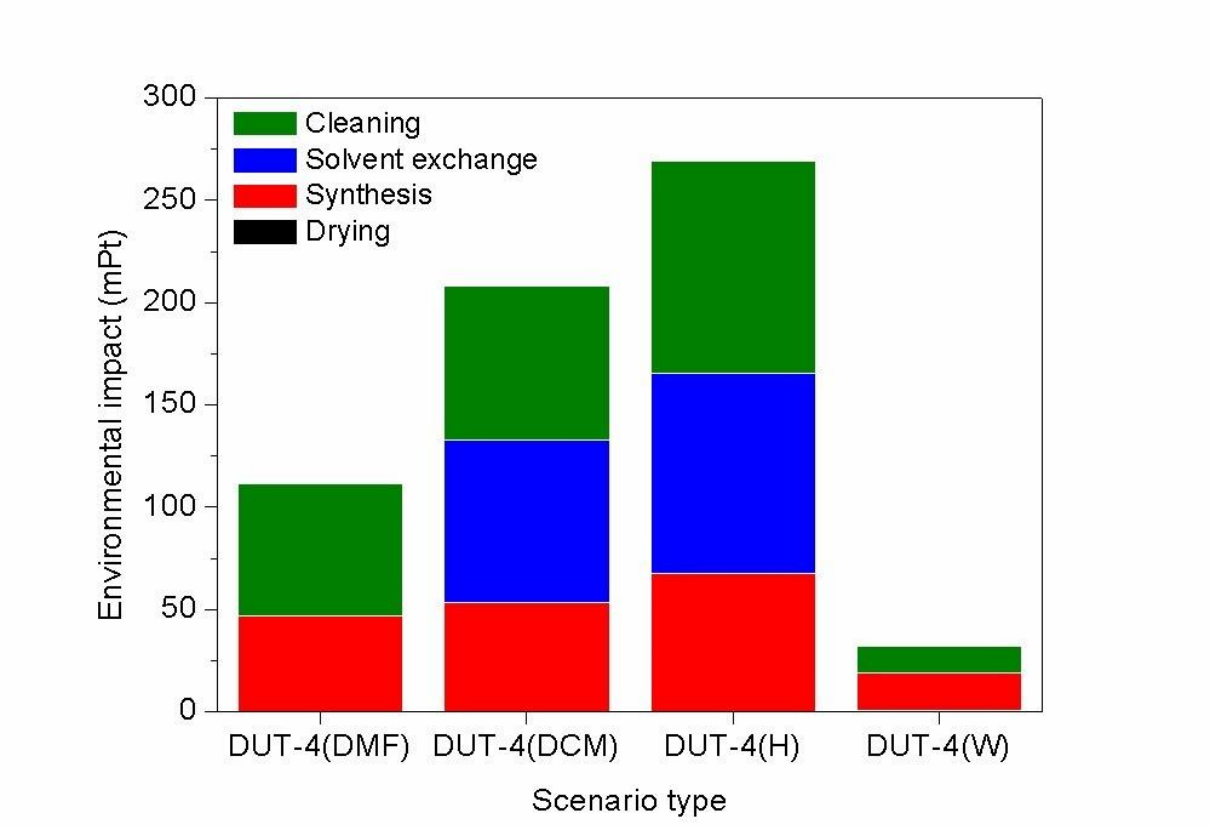

Figure 7. Environmental impact of each Scenario of DUT-4 production through ReCiPe 2016 endpoint method.

The Scenario DUT-4(DCM) has similar behavior to the Scenario DUT-4(H), but a lower environmental impact (211.07 mPt) since it uses 29 % and 7 % less DMF and DCM, respectively, and hexane is not used (Table 1). The production of DUT-4 only uses DMF as the

solvent, and its environmental impact is 112 mPt (less than half of Scenario DUT-4(H)). The solvent used determines the environmental profile of these adsorbents. Similar results were found by Grande et al.[22], who evaluated the LCA of the MOF CPO-27, concluding that solvents used in the synthesis and the cleaning stages have the most significant environmental damage. The authors reduced the environmental impact up to 100 times through water-based synthesis since water is non-toxic, stable, cheap, and readily available [44].

In Scenario DUT-4(W), deionized water as the solvent, cause minimum environmental damage, 32 mPt. In this Scenario, the electricity used in the synthesis and cleaning stages (Table 1) accounts for 97 % of the environmental indicator. México's energy primary source for electricity production is 87 % fossil sources (62 % crude oil, 20 % natural gas, 4 % coal, and the remaining condensates) [52].

As shown in Figure 8, the main environmental impact category indicator in all Scenarios of DUT-4 production is fossil depletion (10.71–109.14 mPt); this is mainly due to solvent production. In terms of fossil depletion midpoint indicator, the solvent used in each Scenario have impacts of 1.86×10^{-4}, 0.28, 0.53, and 0.75 kg oil eq for scenarios DUT-4(W), DUT-4(DMF), DUT-4(DCM), and DUT-4(H), respectively; and an electricity consumption <0.08 kg oil eq for all scenarios (Table S4).

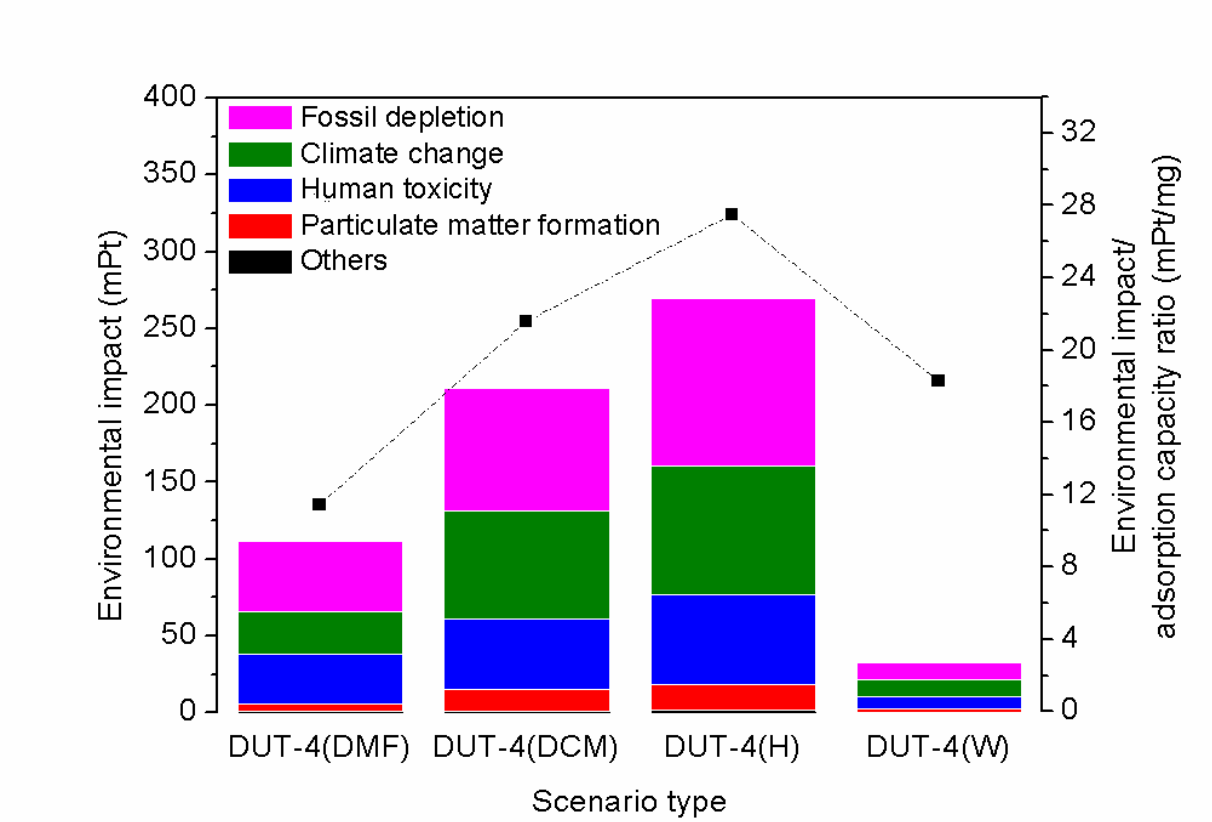

Figure 8. LCA for different DUT-4 production scenarios through endpoint using SimaPro software.

The second most representative indicator is climate change (11.34–83.10 mPt). Regarding the midpoint indicator, the GHG emissions account for 0.25–2.02 kg CO_2 eq (Table S3), mostly associated with carbon dioxide and methane emission. As in the case of fossil depletion indicator, solvents production is the activity with the most incidence in GHG emissions, 7.23×10^{-4}, 0.45, 1.50, and 1.83 kg CO_2 eq for Scenarios DUT-4(W), DUT-4(DMF), DUT-4(DCM), and DUT-4(H), respectively, while electricity consumption generated <0.24 kg CO_2 eq (Table S4).

The human toxicity indicator in Figure 8 ranges between 7.48–58.70 mPt, equivalent to 0.01–0.42 kg 1,4-DB eq. Similarly, solvents use is the main activity of this environmental damage. For the solvent production, pour barium into water represents 81.4–84.7 % of this indicator, and

emitting selenium into the air accounts for 3.1–4.4 %, while the electricity consumption generates <2.6 % in each Scenario. The particulate matter formation indicator (2.59–16.72 mPt) comes mainly from the air emissions in solvent production: $PM_{2.5}$ (1.44–4.20 mPt), sulfur dioxide (0.64–5.41 mPt), and nitrogen oxides (0.32–4.30 mPt).

Similar results were obtained by Loya-González et al. [20] and Sepúlveda Cervántes et al. [21], where the leading environmental indicators were fossil depletion (~55 and 42 %, respectively), climate change (~33 and ~36 %, respectively), and particulate matter formation (~11 and ~10 %, respectively).

It is possible to observe that the substitution of DMF solvent for water, during the synthesis of DUT-4(DMF), diminishes environmental damage—Scenario DUT-4(W)—but this substitution changed the physicochemical properties of the original MOF, having as a consequence a low siloxane adsorption capacity in the biogas purification. This matter deserves to be analyzed from an environmental perspective.

The environmental impact/adsorption capacity ratio was calculated for the four different DUT-4 production scenarios (right axis in Figure 8). The DUT-4(H) adsorbent production has the highest significant environmental impact/adsorption capacity ratio among all four DUT-4 scenarios. In contrast, the DUT-4(DMF) production scenario has the lowest environmental impact/adsorption capacity ratio. These results can be explained by taking into account that DUT-4(DMF) and DUT-4(H) have the same adsorption capacity, but the latter has a higher environmental impact caused by the two solvent exchange stages. Instead, the DUT-4(W) production scenario with a green solvent has a higher environmental impact/adsorption capacity ratio than DUT-4(DMF) production. This result can be explained considering that DUT-4(W)

has the lowest siloxane adsorption capacity; thus, to achieve similar adsorption than the rest (around 9.80 mg/g), it is necessary to produce five times more of this material. This fact could lead to economic savings to foster greater sustainability in removing siloxanes from biogas. From an environmental and technical point of view, DUT-4(DMF) is the best Scenario to produce the siloxane adsorbent since the ratio obtained was 53, 42, and 63 % lower than DUT-4(DCM), DUT-4(H), and DUT-4(W), respectively.

CONCLUSIONS

In this study, the synthesis of DUT-4 was carried out by four different routes to improve its physicochemical characteristics for higher siloxane D4 adsorption. In addition, the environmental impacts of the different routes were evaluated by the life cycle assessment methodology.

According to the physicochemical analysis, only the solvothermal synthesis produced materials isostructural to DUT-4 and favors high specific surface areas with values higher than 1100 m^2/g. The experimental data demonstrated DUT-4 to be a suitable candidate for use as an adsorbent to remove siloxane from gaseous streams such as biogas. The life cycle assessment emphasizes that using DMF, DCM, and hexane increases environmental damage, mainly in the indicators of fossil depletion, climate change, and human toxicity. Therefore, the synthesis of DUT-4(W) was the one with the lowest environmental impact. However, DUT-4(W) presented the lowest siloxane adsorption capacity compared to DUT-4(DMF), DUT-4(DCM), and DUT4(H). Finally, based on the environmental impact/adsorption capacity ratio, the Scenario DUT-4(DMF) production is the most convenient since lower adsorbent mass is required to remove siloxane, which reduces the environmental impacts of the adsorption process.

ASSOCIATED CONTENT

Supporting Information

PDF files containing details of the calculation of the energy balance, estimation methods, environmental impact categories, description of the indicators of fossil depletion, and climate change.

AUTHOR INFORMATION

Corresponding Author

* Nancy Elizabeth Dávila-Guzmán

Phone number: 52-8183294000, ext. 3475

Fax number: 52-8183294000, ext. 6282

E-mail: nancy.davilagz@uanl.edu.mx

* Pasiano Rivas García

E-mail: pasiano.rivasgr@uanl.edu.mx

Author Contributions

The manuscript was written through contributions of all authors. All authors have given approval to the final version of the manuscript.

Notes

The authors declare no competing financial interest.

ACKNOWLEDGMENT

We would like to gratefully acknowledge Facultad de Ciencias Quimicas, UANL (PAICYT-UANL Project No IT1297-20) and Consejo Nacional de Ciencia y Tecnologia de Mexico (Scholarship number 781451). As well as the financial support received from the Consejo Nacional de Ciencia y Tecnologia (CONACyT), under project CB-2015-254294. Sandra Pioquinto is grateful for the support of Melissa Itzel Sánchez Alvarado and Alan A. Rico-Barragán.

REFERENCES

[1] S. Yusup *et al.*, "Emerging Technologies for Biofuels Production," in *Biofuels: Alternative Feedstocks and Conversion Processes for the Production of Liquid and Gaseous Biofuels*, Elsevier, 2019, pp. 45–76. doi: 10.1016/B978-0-12-816856-1.00002-6.

[2] A. Bomboí, "Pretratamiento del biogás procedente de la digestión anaerobia de lodos de EDARs para su posterior valorización energética," Madrid, España. Accessed: Mar. 25, 2020. [Online]. Available: http://www.ategrus.org/wp-content/uploads/2015/05/4-Ponencia-Arantxa-Bombo%C3%AD-EDAR-Pretratamiento-Biog%C3%A1s.pdf

[3] E. Santos-Clotas, A. Cabrera-Codony, E. Boada, F. Gich, R. Muñoz, and M. J. Martín, "Efficient removal of siloxanes and volatile organic compounds from sewage biogas by an anoxic biotrickling filter supplemented with activated carbon," *Bioresour. Technol.*, vol. 294, p. 122136, Dec. 2019, doi: 10.1016/j.biortech.2019.122136.

[4] A. Pertiwiningrum, "HEATING VALUE ENHANCEMENT BY BIOGAS PURIFICATION USING NATURAL ZEOLITE AND RICE STRAW-BASED BIOCHAR," *Int. J. GEOMATE*, vol. 16, no. 55, Mar. 2019, doi: 10.21660/2019.55.4715.

[5] E. Santos-Clotas, A. Cabrera-Codony, B. Ruiz, E. Fuente, and M. J. Martín, "Sewage biogas efficient purification by means of lignocellulosic waste-based activated carbons," *Bioresour. Technol.*, vol. 275, pp. 207–215, Mar. 2019, doi: 10.1016/j.biortech.2018.12.060.

[6] J. Álvarez-Flórez and E. Egusquiza, "Analysis of damage caused by siloxanes in stationary reciprocating internal combustion engines operating with landfill gas," *Eng. Fail. Anal.*, vol. 50, pp. 29–38, Apr. 2015, doi: 10.1016/j.engfailanal.2015.01.010.

[7] G. Ruiling, C. Shikun, and L. Zifu, "Research progress of siloxane removal from biogas," *Biol Eng*, vol. 10, p. 10, 2017.

[8] M. Shen, Y. Zhang, D. Hu, J. Fan, and G. Zeng, "A review on removal of siloxanes from biogas: with a special focus on volatile methylsiloxanes," *Environ. Sci. Pollut. Res.*, vol. 25, no. 31, pp. 30847–30862, Nov. 2018, doi: 10.1007/s11356-018-3000-4.

[9] G. Wang, Z. Zhang, and Z. Hao, “Recent advances in technologies for the removal of volatile methylsiloxanes: A case in biogas purification process,” *Crit. Rev. Environ. Sci. Technol.*, vol. 49, no. 24, pp. 2257–2313, Dec. 2019, doi: 10.1080/10643389.2019.1607443.

[10] B. Tansel and S. C. Surita, “Managing siloxanes in biogas-to-energy facilities: Economic comparison of pre- vs post-combustion practices,” *Waste Manag.*, vol. 96, pp. 121–127, Aug. 2019, doi: 10.1016/j.wasman.2019.07.019.

[11] V. T. L. Tran, P. Gélin, C. Ferronato, J. Chovelon, L. Fine, and G. Postole, “Adsorption of linear and cyclic siloxanes on activated carbons for biogas purification: Sorbents regenerability,” *Chem. Eng. J.*, vol. 378, p. 122152, Dec. 2019, doi: 10.1016/j.cej.2019.122152.

[12] L. Yang and S. I. Corsolini, “Online removal of volatile siloxanes in solid-state anaerobic digester biogas using a biofilter and an activated carbon filter,” *J. Environ. Chem. Eng.*, vol. 7, no. 5, p. 103284, Oct. 2019, doi: 10.1016/j.jece.2019.103284.

[13] F. Gándara, “Metal-organic frameworks: nuevos materiales con espacios llenos de posibilidades,” *Quím*, p. 7, 2012.

[14] H. T. D. Nguyen, Y. B. N. Tran, H. N. Nguyen, T. C. Nguyen, F. Gándara, and P. T. K. Nguyen, “A Series of Metal–Organic Frameworks for Selective CO_2 Capture and Catalytic Oxidative Carboxylation of Olefins,” *Inorg. Chem.*, vol. 57, no. 21, pp. 13772–13782, Nov. 2018, doi: 10.1021/acs.inorgchem.8b02293.

[15] V. Kumar, S. Kumar, K.-H. Kim, D. C. W. Tsang, and S.-S. Lee, “Metal organic frameworks as potent treatment media for odorants and volatiles in air,” *Environ. Res.*, vol. 168, pp. 336–356, Jan. 2019, doi: 10.1016/j.envres.2018.10.002.

[16] N. D. Rudd *et al.*, “Highly Efficient Luminescent Metal–Organic Framework for the Simultaneous Detection and Removal of Heavy Metals from Water,” *ACS Appl. Mater. Interfaces*, vol. 8, no. 44, pp. 30294–30303, Nov. 2016, doi: 10.1021/acsami.6b10890.

[17] Y. Mito-oka *et al.*, “Siloxane D4 capture by hydrophobic microporous materials,” *J. Mater. Chem. A*, vol. 1, no. 27, p. 7885, 2013, doi: 10.1039/c3ta11217a.

[18] N. Gargiulo *et al.*, “Chromium-based MIL-101 metal organic framework as a fully regenerable D4 adsorbent for biogas purification,” *Renew. Energy*, vol. 138, pp. 230–235, Aug. 2019, doi: 10.1016/j.renene.2019.01.096.

[19] E. Haya Leiva, “Análisis de Ciclo de Vida.” Creative Commons, 2016.

[20] D. Loya-González *et al.*, “Optimal activated carbon production from corn pericarp: A life cycle assessment approach,” *J. Clean. Prod.*, vol. 219, pp. 316–325, May 2019, doi: 10.1016/j.jclepro.2019.02.068.

[21] C. V. Sepúlveda-Cervantes, E. Soto-Regalado, P. Rivas-García, M. Loredo-Cancino, F. dJ Cerino-Córdova, and R. B. García Reyes, “Technical-environmental optimisation of the activated carbon production of an agroindustrial waste by means response surface and life cycle assessment,” *Waste Manag. Res.*, vol. 36, no. 2, pp. 121–130, Feb. 2018, doi: 10.1177/0734242X17741680.

[22] C. A. Grande, R. Blom, A. Spjelkavik, V. Moreau, and J. Payet, "Life-cycle assessment as a tool for eco-design of metal-organic frameworks (MOFs)," *Sustain. Mater. Technol.*, vol. 14, pp. 11–18, Dec. 2017, doi: 10.1016/j.susmat.2017.10.002.

[23] I. Senkovska, F. Hoffmann, M. Fröba, J. Getzschmann, W. Böhlmann, and S. Kaskel, "New highly porous aluminium based metal-organic frameworks: Al(OH)(ndc) (ndc=2,6-naphthalene dicarboxylate) and Al(OH)(bpdc) (bpdc=4,4′-biphenyl dicarboxylate)," *Microporous Mesoporous Mater.*, vol. 122, no. 1–3, pp. 93–98, Jun. 2009, doi: 10.1016/j.micromeso.2009.02.020.

[24] "ISO 14044:2006(es), Gestión ambiental — Análisis del ciclo de vida — Requisitos y directrices." https://www.iso.org/obp/ui/#iso:std:iso:14044:ed-1:v1:es (accessed Apr. 16, 2020).

[25] "ecoQuery - Login." https://ecoquery.ecoinvent.org/Account/LogOn?ReturnUrl=%2fFile%2fReports (accessed May 23, 2020).

[26] E. Ramírez Lara *et al.*, "A comprehensive hazardous waste management program in a Chemistry School at a Mexican university," *J. Clean. Prod.*, vol. 142, pp. 1486–1491, 2017, doi: 10.1016/j.jclepro.2016.11.158.

[27] M. Z. Hauschild, R. K. Rosenbaum, and S. I. Olsen, Eds., *Life Cycle Assessment*. Cham: Springer International Publishing, 2018. doi: 10.1007/978-3-319-56475-3.

[28] M. A. J. Huijbregts *et al.*, "ReCiPe2016: a harmonised life cycle impact assessment method at midpoint and endpoint level," *Int. J. Life Cycle Assess.*, vol. 22, no. 2, pp. 138–147, Feb. 2017, doi: 10.1007/s11367-016-1246-y.

[29] T. G. Glover and M. Bin, *Gas Adsorption in Metal-Organic Frameworks: Fundamentals and Applications*, First. Boca Raton. Accessed: Jan. 18, 2021. [Online]. Available: https://books.google.com.mx/books?id=HwprDwAAQBAJ&pg=PT522&lpg=PA1&focus=viewport&hl=es#v=onepage&q&f=false

[30] J. F. Kurisingal *et al.*, "Porous aluminum-based DUT metal-organic frameworks for the transformation of CO2 into cyclic carbonates: A computationally supported study," *Catal. Today*, vol. 352, pp. 227–236, Aug. 2020, doi: 10.1016/j.cattod.2019.12.038.

[31] H. Embrechts, M. Kriesten, M. Ermer, W. Peukert, M. Hartmann, and M. Distaso, "*In situ* Raman and FTIR spectroscopic study on the formation of the isomers MIL-68(Al) and MIL-53(Al)," *RSC Adv.*, vol. 10, no. 13, pp. 7336–7348, 2020, doi: 10.1039/C9RA09968A.

[32] "11.5: Infrared Spectra of Some Common Functional Groups," *Chemistry LibreTexts*, Feb. 09, 2016. https://chem.libretexts.org/Bookshelves/Organic_Chemistry/Map%3A_Organic_Chemistry_(Wade)/11%3A_Infrared_Spectroscopy_and_Mass_Spectrometry/11.05%3A_Infrared_Spectra_of_Some_Common_Functional_Groups (accessed Aug. 18, 2020).

[33] F. Rojo Callejas, "Tablas de Espectroscopía Infrarroja." http://depa.fquim.unam.mx/amyd/archivero/TablasIR_34338.pdf (accessed Aug. 18, 2020).

[34] A. E. J. Hoffman *et al.*, "Elucidating the Vibrational Fingerprint of the Flexible Metal–Organic Framework MIL-53(Al) Using a Combined Experimental/Computational Approach," *J. Phys. Chem. C*, vol. 122, no. 5, pp. 2734–2746, Feb. 2018, doi: 10.1021/acs.jpcc.7b11031.

[35] "IR: carboxylic acids." https://orgchemboulder.com/Spectroscopy/irtutor/carbacidsir.shtml (accessed Aug. 18, 2020).

[36] G. A. Rosales-Sosa *et al.*, "High Elastic Moduli of a 54Al2O3-46Ta2O5 Glass Fabricated via Containerless Processing," *Sci. Rep.*, vol. 5, no. 1, Dec. 2015, doi: 10.1038/srep15233.

[37] P. Benito, F. M. Labajos, L. Mafra, J. Rocha, and V. Rives, "Carboxylate-intercalated layered double hydroxides aged under microwave–hydrothermal treatment," *J. Solid State Chem.*, vol. 182, no. 1, pp. 18–26, Jan. 2009, doi: 10.1016/j.jssc.2008.09.015.

[38] C. Volkringer *et al.*, "The use of aluminium and others p elements (gallium, indium) for the generation of MOF-type materials," in *Studies in Surface Science and Catalysis*, vol. 174, Elsevier, 2008, pp. 447–450. doi: 10.1016/S0167-2991(08)80237-6.

[39] A. Vyalikh, K. Zesewitz, and U. Scheler, "Hydrogen bonds and local symmetry in the crystal structure of gibbsite: Hydrogen bonds and local symmetry in structure of gibbsite," *Magn. Reson. Chem.*, vol. 48, no. 11, pp. 877–881, Nov. 2010, doi: 10.1002/mrc.2682.

[40] J. Ma, A. P. Kalenak, A. G. Wong-Foy, and A. J. Matzger, "Rapid Guest Exchange and Ultra-Low Surface Tension Solvents Optimize Metal-Organic Framework Activation," *Angew. Chem. Int. Ed.*, vol. 56, no. 46, pp. 14618–14621, Nov. 2017, doi: 10.1002/anie.201709187.

[41] J. A. Kaduk and J. T. Golab, "Structures of 2,6-disubstituted naphthalenes," *Acta Crystallogr. B*, vol. 55, no. 1, pp. 85–94, Feb. 1999, doi: 10.1107/S0108768198008945.

[42] B. Zhang *et al.*, "Solvent determines the formation and properties of metal-organic framework," p. 7, 2012.

[43] A. J. Howarth, A. W. Peters, N. A. Vermeulen, T. C. Wang, J. T. Hupp, and O. K. Farha, "Best Practices for the Synthesis, Activation, and Characterization of Metal–Organic Frameworks," *Chem. Mater.*, vol. 29, no. 1, pp. 26–39, Jan. 2017, doi: 10.1021/acs.chemmater.6b02626.

[44] C. Duan *et al.*, "Water-based routes for synthesis of metal-organic frameworks: A review," *Sci. China Mater.*, vol. 63, no. 5, pp. 667–685, May 2020, doi: 10.1007/s40843-019-1264-x.

[45] A. Maskara and D. M. Smith, "Agglomeration during the Drying of Fine Silica Powders, Part II: The Role of Particle Solubility," *J. Am. Ceram. Soc.*, vol. 80, no. 7, pp. 1715–1722, Jan. 2005, doi: 10.1111/j.1151-2916.1997.tb03044.x.

[46] H. L. Lim, K. P. Hapgood, and B. Haig, "Understanding and preventing agglomeration in a filter drying process," *Powder Technol.*, vol. 300, pp. 146–156, Oct. 2016, doi: 10.1016/j.powtec.2016.03.003.

[47] S. Pioquinto García *et al.*, "Siloxane removal for biogas purification by low cost mineral adsorbent," *J. Clean. Prod.*, p. 124940, Nov. 2020, doi: 10.1016/j.jclepro.2020.124940.

[48] "ReCiPe | PRé Sustainability." https://www.pre-sustainability.com/recipe (accessed May 23, 2020).

[49] K. Hjaila, R. Baccar, M. Sarrà, C. M. Gasol, and P. Blánquez, "Environmental impact associated with activated carbon preparation from olive-waste cake via life cycle assessment," *J. Environ. Manage.*, vol. 130, pp. 242–247, Nov. 2013, doi: 10.1016/j.jenvman.2013.08.061.

[50] J. B. Guinee, *Handbook on Life Cycle Assessment. Operational Guide to the ISO Standards*. Netherlands.

[51] S. L. Y. Tang, R. L. Smith, and M. Poliakoff, "Principles of green chemistry: PRODUCTIVELY," *Green Chem.*, vol. 7, no. 11, p. 761, 2005, doi: 10.1039/b513020b.

[52] "SENER | Sistema de Información Energética | Producción de energía primaria." http://sie.energia.gob.mx/bdiController.do?action=cuadro&cvecua=IE11C01 (accessed Sep. 23, 2020).

Graphical abstract:

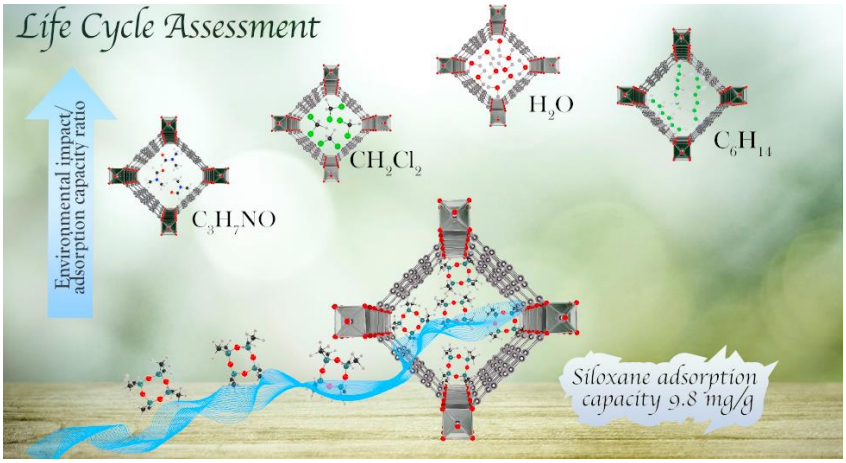

Synopsis: Search of sustainable routes for the synthesis of metal-organic frameworks for clean energy applications.